Available online at www.sciencedirect.com

SciVerse ScienceDirect

Ceramics International 38 (2012) 2679–2684

CERAMICS INTERNATIONAL

www.elsevier.com/locate/ceramint

Ordered domains in lead free $0.94(Na_{0.5}Bi_{0.5})TiO_3$–$0.06BaTiO_3$ ceramics

Liu Yunfei *, Lu Yinong *, Pan Zhigang

State Key Laboratory of Materials-Oriented Chemical Engineering, College of Materials Science and Engineering, Nanjing University of Technology, Nanjing 210009, China

Received 1 November 2011; received in revised form 14 November 2011; accepted 14 November 2011
Available online 22 November 2011

Abstract

The microstructure of lead-free $0.94(Na_{0.5}Bi_{0.5})TiO_3$–$0.06BaTiO_3$ (BNBT-6) piezoelectric ceramics was investigated by different analysis techniques. X-ray diffraction (XRD) result reveals the coexistence of rhombohedral and tetragonal symmetry in the structure of BNBT-6 ceramics at room temperature. Selected area electron diffraction (SAED) patterns reveal the presence of ordered domains in BNBT-6 ceramics. The superlattice reflections $\{h+1/2\,k+1/2\,0\}$ and $\{h+1/2\,k+1/2\,l+1/2\}$ of ordered domains mainly come from the octahedral tilt and chemical ordering of A-site atoms. High-resolution transmission electron microscopy (HRTEM) combined with image processing is an effective method to investigate the defects and the size of ordered domains in BNBT-6 ceramics. One-dimensional fringe images of superlattice reflections indicate that there are significant local Na and Bi atomic layer displacements and anti-phase boundaries as a result of chemical ordering, which provide a driving force for order–disorder transformation. A filtered HRTEM black/white image shows the size of ordered domains to be about 5–10 nm.

Keywords: HRTEM; Superlattice reflection; Ordered domain; Antiphase boundary

1. Introduction

In recent years, much interest has been focused on lead-free piezoelectric materials based on the viewpoint of environment impact. Since Smolenskii [1] reported that the A-site complex perovskite compound $Na_{0.5}Bi_{0.5}TiO_3$ (NBT) has piezoelectric properties, this material as a key lead-free piezoelectric ceramics to substitute PZT based materials and PMN based relaxor ferroelectrics, has aroused extensive interest of researchers [2–8]. Most of the previous researches about NBT or NBT based complex perovskite ceramics, however, concentrated on the improvement of piezoelectric properties and the temperature induced phase transitions. Takenaka et al. reported that $Na_{0.5}Bi_{0.5}TiO_3$–$BaTiO_3$ (BNBT) showed the highest piezoelectric constant with composition close to the morphotropic phase boundary (MPB) [2]. Yilmaz [3] synthesized textured BNBT (5.5 mol% $BaTiO_3$) ceramics using templated grain growth method (TGG) showing piezoelectric constant d_{33} = 520 pC/N (high field) which is higher than that of single crystal of BNBT (6.0 mol% $BaTiO_3$, d_{33} = 450 pC/N) [4]. Summarizing previous studies, NBT and NBT based complex perovskite ceramics undergo two-phase transitions, i.e., cubit ↔ tetragonal at ~540 °C and tetragonal ↔ rhombo-rhombohedral at ~250 °C [2,4,5]. Liu et al. also reported that BNBT ceramics experience one structural phase transition and two ferroelectric phase transitions under 400 °C: tetragonal paraelectric phase ↔ tetragonal antiferroelectric phase ↔ rhombohedral (or rhombohedral plus tetragonal) ferroelectric phase [6].

It is well known that BNBT ceramics are relaxor ferroelectrics, which show diffuse phase transition and a frequency dependent dispersion behavior with suitable $BaTiO_3$ contents [9]. Most of the relaxor ferroelectrics having the general formula $A(B'B'')O_3$ show high dielectric and piezoelectric constants, which indicates that the behaviors and properties of these materials have a very close relationship with the order–disorder transition and the ordering degree of the complex perovskite structure [10]. Wang et al. summarized that the formation of ordered structure is strongly dominated by the differences in both valence and ionic radii between the B′ and B″ cations in most complex $A(B'B'')O_3$ perovskites [11]. Previous researches ascribed the origin of ordered domains due to the localized chemical ordering in relaxor materials, such as

* Corresponding authors. Tel.: +86 25 8317218; fax: +86 25 8317218.
E-mail addresses: yfliu@njut.edu.cn, lyf2225@163.com (L. Yunfei), ynlu@njut.edu.cn (L. Yinong).

0272-8842/$36.00
doi:10.1016/j.ceramint.2011.11.035

lead scandium tantalite (PST) and lead magnesium niobate (PMN) [12,13]. Since BNBT ceramics with the general formula $(A'A'')BO_3$ are regarded as the relaxor ferroelectrics, they may have ordered structure in theory. But the difference in ionic radii between Na^+ and Bi^{3+} is insignificant based on Wang report [11], the tendency for ordering is slight. Consequently the microstructure of BNBT ceramics needs to be investigated in detail to reveal whether it has ordering characteristics or not.

In this study, BNBT ceramics for the composition of the MPB (6.0 mol% $BaTiO_3$) were synthesized by solid-state preparation method. The microstructure, including ordered domain, displacement, anti-phase boundary and so on, was investigated by a combination of XRD, SAED, and HRTEM techniques. The mechanism of superlattice reflection formation in BNBT ceramics was discussed by virtue of HRTEM images and SAED patterns.

2. Experimental procedure

To synthesize the BNBT-6 ceramics, high purity raw materials Bi_2O_3 (99.9%), TiO_2 (99.0%), Na_2CO_3 (99.8%), and $BaTiO_3$ (99.0%) were mixed with composition $0.94(Bi_{0.5}Na_{0.5})TiO_3$–$0.06BaTiO_3$ by ball milling for 20 h. Then the dried powders were calcined at 850 °C for 2 h in air. The calcined powders were re-milled for 16 h and dried, and then were cold-pressed at 160 MPa into discs of approximately Ø13 mm diameter and 2 mm thickness. Finally, the discs were sintered at 1150 °C for 2 h.

The structure characteristics and phase purity of the sintered BNBT-6 ceramics were identified by XRD using an ARL X'TRA diffractometer (Themo Electron Co., Ecublens, Switzerland) with CuKα (λ = 1.5406 Å) radiation, in continuous scan mode with 0.5°/min in the range of 10–80° (2θ). For HRTEM and SAED observation, the specimen was first polished to about 100 μm in thickness and ultrasonically cut into a disc of Ø3 mm in diameter, and then the disc was dimple grinded to about 20 μm in thickness. The final perforation in the disc center was performed using argon ions from both sides via Precision Ion Polishing System (PIPS, Model 691, GATAN Co., Pleasanton, CA). The microstructure characteristics and SAED were conducted with a HRTEM (JEM-2010, JEOL) equipped with a side-entry double-tilting specimen holder. Image filtering and processing were conducted by DigitalMicrographa software (GATAN).

3. Results and discussion

3.1. XRD characterization

Fig. 1 shows the XRD pattern of BNBT-6 ceramics that exhibits a single perovskite structure, and there are no other phases like pyrochlore structure. All reflections in the case were indexed on the basis of the pseudocubic perovskite unit cell. The pattern clearly shows rhombohedral split (see inset of Fig. 1), which means that the structure of BNBT-6 ceramics is pseudocubic with a very small deviation from ideal cubic symmetry. In other words, under the effect of the excess $BaTiO_3$ (6.0 mol%), the structure of BNBT-6 is the coexistence of rhombohedral and tetragonal symmetry at room temperature. Measurement results show that rhombohedral structure has cell parameter $a = 3.9013$ Å, $\alpha = 89.688°$, and tetragonal structure has cell parameter $a = 3.9028$ Å, $c = 3.9205$ Å, respectively.

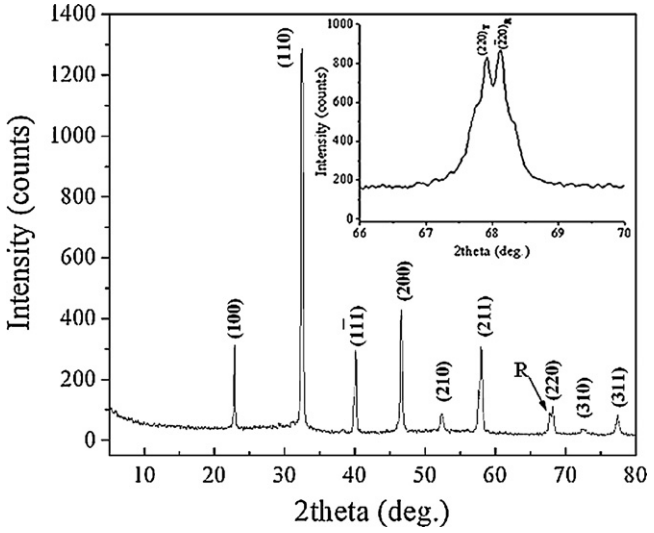

Fig. 1. XRD pattern of BNBT-6 ceramics, R denotes rhombohedral split.

Based on Soukhojak report [14], ordered domains occur in BNBT crystal. No ordered domain reflections, however, can be observed in the XRD pattern of BNBT-6 ceramics besides rhombohedral split. There are two possible reasons for the limitation of ordered domain reflections. One is the heavy X-ray absorption that masks the weak ordered domains lines, and the other is the small size of ordered domains that cannot be detected by XRD. Therefore, in order to validate whether there are ordered domains in BNBT-6 ceramics or not, the electron microscopy was processed.

3.2. SAED characterization

Fig. 2 shows three kinds of SAED patterns from the studied specimen that were observed along [0 0 1], [1 1 1], and [0 1 1] zone axis directions via rotating the double-tilting specimen holder, respectively. In [0 0 1] and [1 1 1] zone axis directions, Fig. 2(a) and (b), the diffraction patterns show the existence of $\{h + 1/2\, k + 1/2\ \ 0\}$ superlattice reflections (indicated by the empty arrow). And in [0 1 1] zone axis diffraction pattern, Fig. 2(c), the diffraction pattern shows another kind of superlattice reflections $\{h + 1/2\, k + 1/2\, l + 1/2\}$ in all three directions, and the intensities of superlattice reflections are stronger than $\{h + 1/2\, k + 1/2\ \ 0\}$ superlattice reflections. The presence of superlattice reflections confirmed that there are ordered domains in BNBT-6 ceramics.

For the origin of superlattice formation in complex perovskite, there are mainly three possible mechanisms [14]: (1) chemical ordering of the species, (2) octahedral tilt, (3) anti-parallel displacement of ions. For chemical ordering, the characteristic is that the intensities of superlattice reflections do not change significantly with temperature [13]. For NBT single

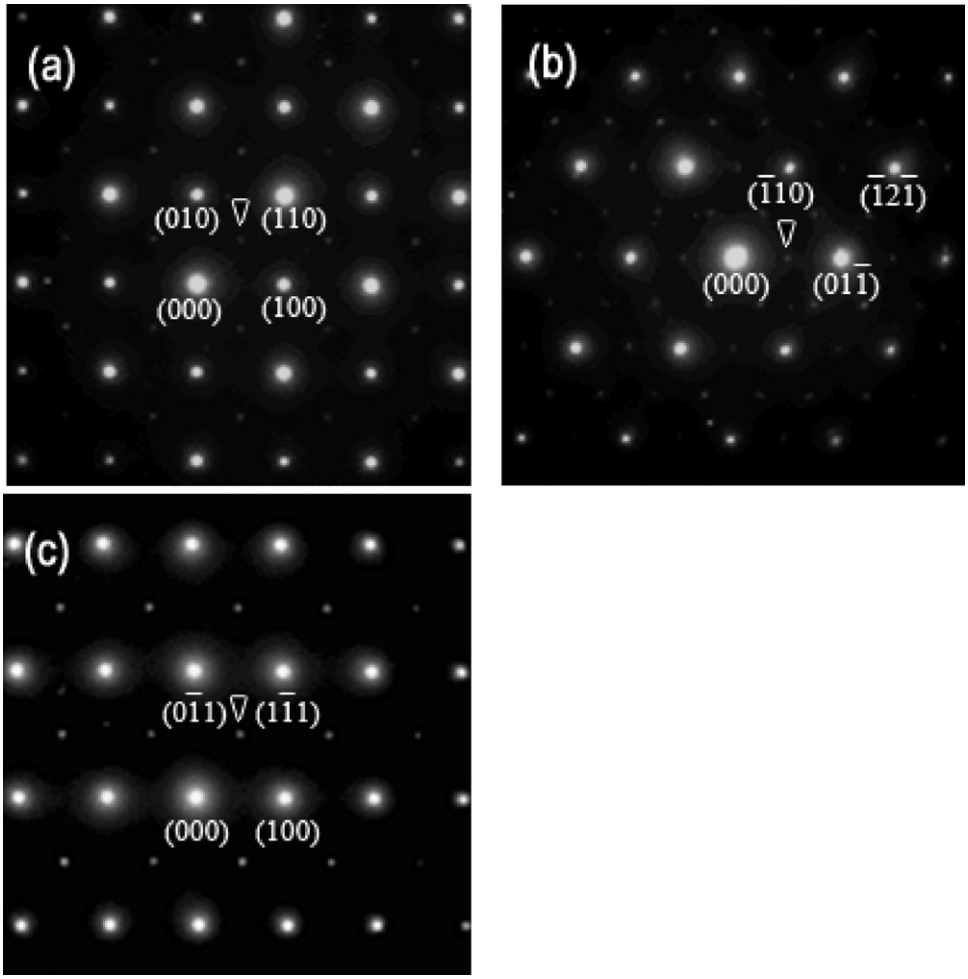

Fig. 2. SAED patterns obtained from BNBT-6 ceramics, along zone axis (a) [0 0 1], (b) [1 1 1] and (c) [0 1 1] directions, respectively. Superlattice reflections are indicated by empty arrows.

crystal, the intensities of $\{h+1/2\,k+1/2\ \ 0\}$ superlattice reflections vary with temperature, and almost completely vanish under 700 °C, so superlattice reflections $\{h+1/2\,k+1/2\ \ 0\}$ in NBT single crystal caused by chemical ordering may be excluded [14]. For octahedral tilt, Vakhrushev et al. [15] reported that NBT has tetragonal M_3 superlattice and rhombohedral R_{35} superlattice caused by single axis in-phase tilt ($a^0\,a^0\,c^+$) and three-axis equivalent anti-phase tilt ($a^-\,a^-\,a^-$), respectively. And the tetragonal M_3 superlattice is manifested as $\{h+1/2\,k+1/2\,l\}$ reflections except where $h=k$, and the rhombohedral R_{35} superlattice is manifested as $\{h+1/2\,k+1/2\,l+1/2\}$ reflections except where $h=k=l$. In present case, XRD result indicates that there are coexisting phases of tetragonal and rhombohedral in BNBT-6 ceramics, and at the same time SAED patterns show the superlattice reflections $\{h+1/2\,k+1/2\ \ 0\}$ and $\{h+1/2\,k+1/2\,l+1/2\}$. Therefore, we can determine that octahedral tilt is a driving force of the superlattice formation in BNBT-6 ceramics at least.

Forbiddance for tetragonal superlattice reflection $(1/2\,1/2\,0)$, however, appears on the SAED pattern along [0 0 1] zone axis, which indicates that there are other driving forces for the superlattice formation. We confirmed that chemical ordering of Bi and Na at A-site along [1 1 0] direction and [1 1 1] direction is the other main reason for the superlattice reflections $\{h+1/2\,k+1/2\ \ 0\}$ and $\{h+1/2\,k+1/2\,l+1/2\}$ through HRTEM observation and computer simulation of ordered structural model [16]. And the intensities of $\{h+1/2\,k+1/2\,l+1/2\}$ superlattice reflections are stronger than the $\{h+1/2\,k+1/2\ \ 0\}$ superlattice reflections, which means that the three-axis equivalent anti-phase tilt ($a^-\,a^-\,a^-$) act as the main factors for the formation of ordered domains (superlattice reflections).

3.3. HRTEM observations and image processing

In order to investigate the defects and determine the size of ordered domains, HRTEM was used to form lattice images. The original HRTEM image contains both signal and noise, and the noise usually affects the accurate analysis of HRTEM image. So image-processing technique was used to improve the signal to noise ratio of the image. Fig. 3 demonstrates the image-processing course. Fig. 3(a) is a HRTEM image parallel to the (0 0 1) plane of BNBT-6 ceramics. A fast Fourier

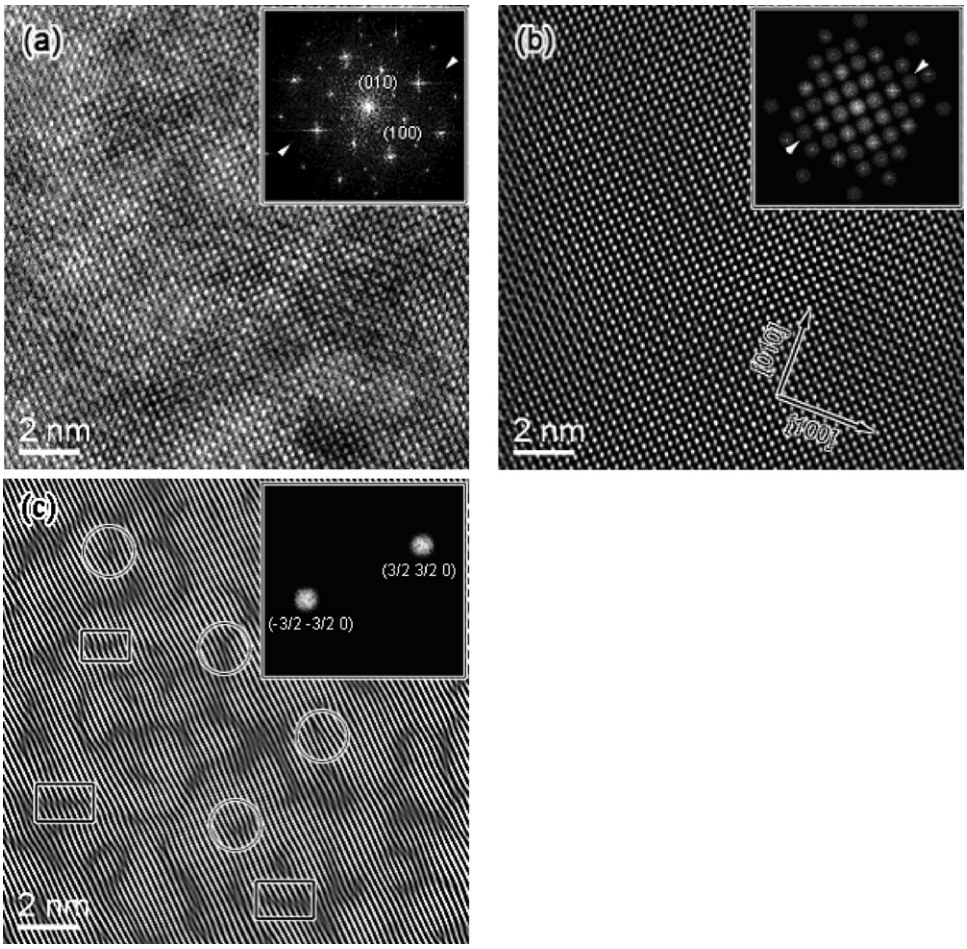

Fig. 3. HRTEM images of BNBT-6 along [0 0 1] zone axis. (a) Original HRTEM image, inset image is the fast Fourier transform (FFT), where superlattice reflections are evident. (b) A Fourier-filter image of (a) using a periodic filter to include both ordered and disordered reflections and exclude noise. (c) A one-dimensional image, where one pair of superlattice reflection spots $(3/2\,3/2\,0)$ and $(\bar{3}/2\,\bar{3}/2\,0)$ were included, showing severe displacements of Na and Bi atom layers (indicated by circles) and anti-phase domain boundaries (indicated by squares).

transformation (FFT) of this image is shown in the inset of Fig. 3(a), and superlattice reflections $\{h+1/2\,k+1/2\;\;0\}$ are evident. Fig. 3(b) is a Fourier filtered image of Fig. 3(a). The filtering process is described in the following. Mask is applied to the FFT pattern to eliminate noise and only keep the masked diffraction spots. Then a reverse FFT is carried out on the filtered FFT pattern to back the real space from reciprocal space, resulting in the improved signal Fourier filtered image. Fig. 3(c) is a one-dimensional image achieved only by the superlattice reflections $(3/2\,3/2\,0)$ and $(\bar{3}/2\,\bar{3}/2\,0)$ in the reciprocal space. The curvature of the fringes characterizes the antiphase domain boundaries (indicated by squares), which are normally associated with an order–disorder transformation [17]. Usually, when chemical ordering occurs in different regions on different sublattices, antiphase boundary defects will be formed when these regions meet [18]. Therefore the intensity of superlattice reflections originated from the scattering of the ordered Na and Bi atoms, and the fringe contrast in Fig. 3(c) should represent the Na, Bi, or (Na + Bi) atom planes. Fig. 4 is the HRTEM image parallel to the (0 1 1) plane of BNBT-6 ceramics acquired by the same image processing. One-dimensional image achieved by $(3/2\,\bar{3}/2\,3/2)$ and $(\bar{3}/2\,3/2\,\bar{3}/2)$ superlattice reflections also shows the antiphase domain boundaries. In addition, the displacements (indicated by circles) of the local Na and Bi atom layers can also be found in Figs. 3(c) and 4(b). Based on the above analysis, in this case, chemical ordering is the other driving force for both $\{h+1/2\,k+1/2\;\;0\}$ and $\{h+1/2\,k+1/2\,l+1/2\}$ superlattice formations in BNBT-6 ceramics. And the displacements of the local Na and Bi atom layers also affect the formation of ordered domains.

As mentioned above, SAED patterns indicate that there are ordered domains in BNBT-6 ceramics on the basis of superlattice reflections. However, SAED cannot be used to unambiguously discern between the degree of ordering and the size of ordered domains, because the degree of ordering within the ordered domains is not known. In order to determine the size of ordered domains in disordered BNBT-6 matrix, the HRTEM image processing was conducted again. Fig. 5 demonstrates the process to differentiate the nanosized ordered domains and the disordered matrix. Fig. 5(a) shows a Fourier filtered HRTEM image, which has both ordered and disordered reflections. Fig. 5(b) and (c) shows the high-magnification HRTEM images about region A and region B in Fig. 5(a), respectively. From

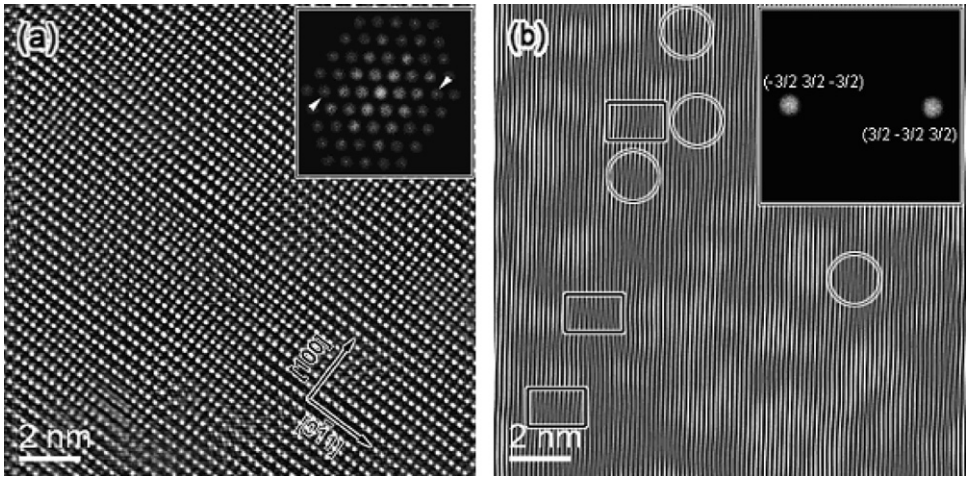

Fig. 4. (a) A Fourier-filter image using a periodic filter to include both ordered and disordered reflections along [0 1 1] zone axis direction. (b) A one-dimensional image, where one pair of superlattice reflection spots $(3/2\,\bar{3}/2\,3/2)$ and $(\bar{3}/2\,3/2\,\bar{3}/2)$ were included, showing severe displacements of Na and Bi atom layers (indicated by circles) and anti-phase domain boundaries (indicated by squares).

Fig. 5(b) and (c), ordered domains are clearly distinguished from the disordered matrix, the pseudo-hexagonal regions correspond to the ordered phase and the tetragonal or fringe regions correspond to the disordered phase [19,20]. Fig. 5(d) is a filtered image, where only $\{h + 1/2\,k + 1/2\,l + 1/2\}$ superlattice reflections were selected in the Fourier reciprocal space, but it was converted to a black/white image, where the ordered domains are clearly distinguished from the disordered matrix

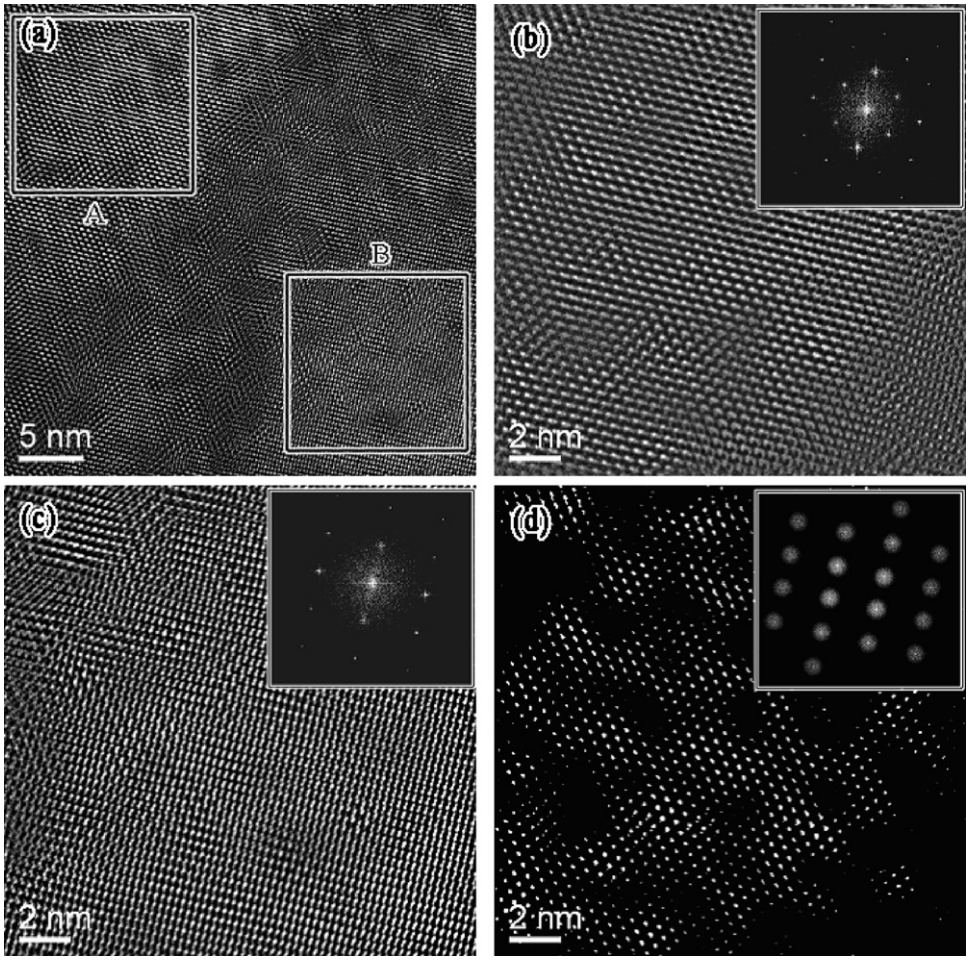

Fig. 5. (a) A HRTEM image including ordered and disordered regions. (b) A high-magnification HRTEM image about region A, mainly showing the ordered domains. (c) A high-magnification HRTEM image about region A, mainly showing the disordered domains. (d) A black/white image showing the size of the ordered domains.

(black background). And the size of ordered domains is about 5–10 nm.

4. Conclusions

Microstructure of BNBT-6 ceramics, including ordered domain, anti-phase boundary, and displacement, was investigated by XRD, SAED, and HRTEM. SAED patterns and HRTEM images reveal the existence of ordered domains in disordered matrix. One-dimensional fringe images obtained by a pair of superlattice reflection spots are curved and distorted. This means that there are significant local Na and Bi atomic layer displacements and anti-phase boundaries. Antiphase boundaries are the result of chemical ordering which is a driving force for the formation of ordered domains. HRTEM combined with image processing is an effective method to investigate the size of ordered domains in BNBT-6 ceramics, and a filtered HRTEM black/white image shows size of ordered domains to be about 5–10 nm in BNBT-6 ceramics.

Acknowledgement

This work was funded by the project ''Priority Academic Program Development of Jiangsu Higher Education Institutions (PAPD)''.

References

[1] G.A. Smolenskii, V.A. Jsupov, A.I. Agranovskaya, N.N. Kainik, New ferroelectrics of complex composition, Phys. Solid State 2 (1961) 2651–2654 (Eng. Trans.).
[2] T. Takenaka, K. Maruyama, K. Sakata, $(Bi_{1/2}Na_{1/2})TiO_3$–$BaTiO_3$ system for lead-free piezoelectric ceramics, Jpn. J. Appl. Phys. 30 (1991) 2236–2239.
[3] H. Yilmaz, Texturing of $Na_{1/2}Bi_{1/2}TiO_3$–$BaTiO_3$ ceramics by templated grain growth, Ph.D. Thesis, Pennsylvania State University, 2002.
[4] Y.M. Chiang, G.W. Farrrey, A.N. Soukhojak, Lead-free high-strain single-crystal piezoelectrics in the alkaline-bismuth-titanate perovskite family, J. Appl. Phys. Lett. 73 (1998) 3683–3685.
[5] S.E. Park, K.S. Hong, Phase relations in the system of $(Na_{1/2}Bi_{1/2})TiO_3$–$PbTiO_3$. I. Structure, J. Appl. Phys. 79 (1996) 383–387.
[6] Y.F. Liu, Y.N. Lü, M. Xu, S.Z. Shi, H.Q. Xu, X.D. Yang, Structure and electric properties of $(1-x)(Bi_{1/2}Na_{1/2})TiO_3$–$xBaTiO_3$ systems, J. Wuhan Univ. Technol. – Mater. Sci. Ed. 22 (2007) 315–319.
[7] K. Kumar, B.K. Singh, M.K. Gupta, N. Sinha, B. Kumar, Enhancement in dielectric and ferroelectric properties of lead free $Bi_{0.5}(Na_{0.5}K_{0.5})_{0.5}TiO_3$ ceramics by Sb-doping, Ceram. Int. 37 (2011) 2997–3004.
[8] Y.H. Lin, P.S. Cheng, C.C. Wu, T.P. Sun, J.J. Lin, C.F. Yang, Properties of RF magnetron sputtered $0.95Bi_{0.5}Na_{0.5}TiO_3$–$0.05BaTiO_3$ thin film, Ceram. Int. 37 (2011) 3765–3769.
[9] J.R. Gomah-pettry, S. Saïd, P. Marchet, J.P. Mercurio, Sodium-bismuth titanate based lead-free ferroelectric materials, J. Eur. Ceram. Soc. 24 (2004) 1165–1169.
[10] X.W. Zhang, Q. Wang, Study of the order–disorder transition in $A(B'B'')O_3$ perovskite type ceramics, J. Am. Ceram. Soc. 74 (1991) 2846–2850.
[11] Z.L. Wang, Z.C. Kong, Functional and Smart Materials: Structural Evolution and Structure Analysis, Plenum Press, New York, 1998.
[12] M.P. Harmer, A. Bahalla, B. Fox, Electron microscopy of ordered domains in lead scandium tantalite $Pb(Sc_{0.5}Ta_{0.5})O_3$, Mater. Lett. 2 (1984) 278–280.
[13] A.D. Hilton, D.J. Barber, C.A. Randall, T.R. Shrout, On short range ordering in the perovskite lead magnesium niobate, J. Mater. Sci. 25 (1990) 3461–3466.
[14] A.N. Soukhojak, G.W. Wang, Y.M. Chiang, Superlattice in single crystal barium-doped sodium bismuth titanate, J. Phys. Chem. Solids 61 (2000) 301–304.
[15] S.B. Vakhrushev, V.A. Isupov, B.E. Kvyatkovsky, N.M. Okuneva, I.P. Pronin, G.A. Smolensky, P.P. Syrnikov, Phase transitions and soft modes in sodium bismuth titanate, Ferroelectrics 63 (1985) 153–160.
[16] Y.F. Liu, Y.N. Lu, S.Z. Shi, M. Xu, Ordered structure of $0.94Bi_{0.5}Na_{0.5}$-TiO_3–$0.06BaTiO_3$ investigated by the high resolution transmission electron microscopy, J. Chin. Ceram. Soc. 36 (2008) 776–782.
[17] E. Goo, R. Sinclair, Displacement boundaries in TiNi alloys, Scripta Metall. 19 (1985) 1257–1259.
[18] G. King, E. Goo, T. Yamamoto, K. Okosuka, Crystal structure and defects of ordered $(Pb_{1-x}Ca_x)TiO_3$, J. Am. Ceram. Soc. 71 (1988) 454–460.
[19] Z.C. Kang, C. Caranoni, I. Siny, G. Nihoul, C. Boulesteix, Study of the ordering of Sc and Ta atoms in Pb_2ScTaO_6 by X-ray diffraction and high resolution electron microscopy, Nature 346 (1990) 308–320.
[20] H.Z. Jin, J. Zhu, S. Miao, X.W. Zhang, Z.Y. Cheng, Ordered domains and polar clusters in lead magnesium niobate $Pb(Mg_{1/3}Nb_{2/3})O_3$, J. Appl. Phys. 89 (2001) 5048–5052.